Data in Brief 31 (2020) 105708

Contents lists available at ScienceDirect

Data in Brief

journal homepage: www.elsevier.com/locate/dib

Data Article

Magnetic resonance sounding dataset of a hard-rock headwater catchment for assessing the vertical distribution of water contents in the subsurface

Nolwenn Lesparre[a,*], Jean-François Girard[b], Benjamin Jeannot[a], Sylvain Weill[a], Marc Dumont[c], Marie Boucher[d], Daniel Viville[a], Marie-Claire Pierret[a], Anatoly Legchenko[d], Frederick Delay[a]

[a] Université de Strasbourg, CNRS, EOST, LHYGES UMR 7517, F-67000 Strasbourg, France
[b] Université de Strasbourg, CNRS, EOST, IPGS UMR 7516, F-67000 Strasbourg, France
[c] Sorbonne Université, CNRS, EPHE, UMR 7619 METIS, F-75005 Paris, France
[d] Univ. Grenoble Alpes, IRD, CNRS, IGE, F-38000 Grenoble, France

ARTICLE INFO

Article history:
Received 27 April 2020
Revised 6 May 2020
Accepted 7 May 2020
Available online 16 May 2020

Keywords:
Hydrogeophysics
Magnetic resonance sounding
Headwater catchment
Hard-rock aquifer
Conditioning parameters of a hydrological model

ABSTRACT

Magnetic Resonance Sounding (MRS) measurements are acquired at 16 stations in the Strengbach headwater catchment (Vosges Mountains – France). These data, rendering the vertical distribution of water contents in the subsurface, are used to show their potential in conditioning a hydrological model of the catchment, as described in the article "Magnetic resonance sounding measurements as posterior information to condition hydrological model parameters: Application to a hard-rock headwater catchment" – Journal of Hydrology (2020). Acquisition protocols follow a free induction decay scheme. Data are filtered by applying a band-pass filter at the Larmor frequency. A filter removing the 50 Hz noise is also applied with the exception of data at a Larmor frequency close to the 50 Hz harmonic. The signal envelopes are then fitted by a decaying exponential function over time to estimate the median characteristic relaxation time of each MRS sounding.

* Corresponding author.
E-mail address: lesparre@unistra.fr (N. Lesparre).

https://doi.org/10.1016/j.dib.2020.105708

Specifications table

Subject	Water Science and Technology
Specific subject area	Magnetic resonance sounding to assess the distribution of water contents in a shallow hard-rock aquifer
Type of data	Table Graph Figure MRS files (.0X, .fX, .inp, .mrm) Metadata file (.pdf)
How data were acquired	Data are acquired in the field using the magnetic resonance sounding Numis^{plus} device system from IRIS instruments.
Data format	Raw Filtered
Parameters for data collection	Eight-shaped loops, made of two squares of 37.5 or 40 m on a side, are placed on the ground for the data acquisition. At each station, data are collected using the free induction decay protocol. At each station, 6 to 7 electromagnetic pulses are injected and 200 to 300 stacks are applied.
Description of data collection	Data are acquired at 16 stations during two campaigns held in April and May 2013.
Data source location	Observatoire Hydro-Géochimique de l'Environnement (http://ohge.unistra.fr), Aubure, France, located between latitudes 48°12'32" - 48°12'55" and longitudes 7°11'25" - 7°12'12"
Data accessibility	Direct URL to data: http://hplus.ore.fr/files/lesparre-et-al-2020-joh-data.tgz
Related research article	Nolwenn Lesparre, Jean-François Girard, Benjamin Jeannot, Sylvain Weill, Marc Dumont, Marie Boucher, Daniel Viville, Marie-Claire Pierret, Anatoly Legchenko, Frederick Delay, 2020. Magnetic resonance sounding measurements as posterior information to condition hydrological model parameters: Application to a hard-rock headwater catchment. Journal of Hydrology 587, 124941. https://doi.org/10.1016/j.jhydrol.2020.124941

Value of the Data

- The datasets are useful to characterize the subsurface water content of headwater catchments and to evaluate the storage properties of hard-rock aquifers.
- Researchers interested in measurements of water contents collected in hard-rock aquifers could be inspired by these datasets. Researchers developing models of magnetic resonance sounding (MRS) responses could also use these datasets to evaluate their model. Researchers interested in hydrological models could, as well, evaluate the capacity of their models to be conditioned by this dataset on subsurface flow patterns.
- The data give an idea of the noise level at the Strengbach site, which also helps testing acquisition protocols that could provide a better signal-to-noise ratio. With regard to the design of time-lapse experiments, the data also provide an insight on the minimum duration of records required to generate MRS signal variations higher than the measured noise.
- MRS datasets collected on mountainous hard-rock environments are still scarce.

1. Data Description

The Magnetic Resonance Sounding (MRS) datasets presented here are that used in [1] for the calibration of a hydrological model applied for simulating transient flow at the catchment

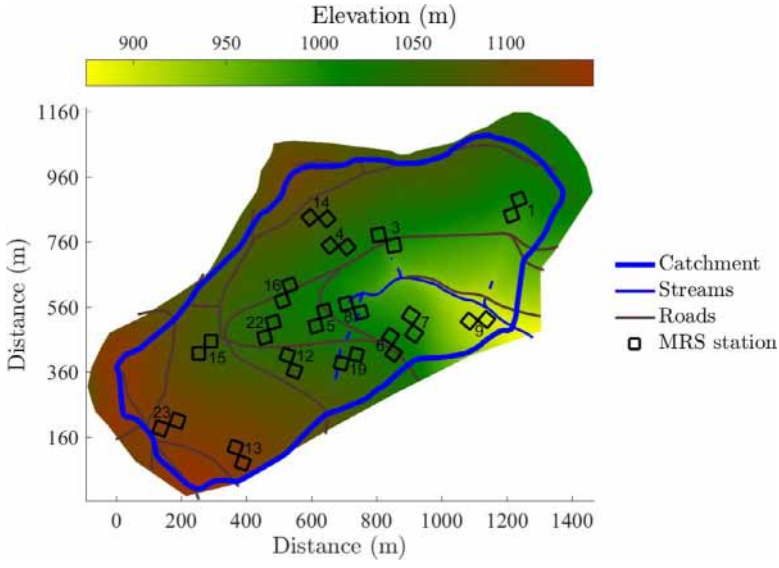

Fig. 1. Location of the MRS stations at the Strengbach catchment.

Table 1
Characteristics of the MRS stations.

Sounding	Site	Latitude (°E)	Longitude (°N)	Acquisition date	Loop size (m)	Files used in ref.[1]
01	Holly 24/25	48°12'55,2974"	7°12'17,9817"	2013/04/12	37,5	.01 to.06 .f1 to.f6
03	Holly 22/23 F7	48°12'52,711"	7°11'58,5495"	2013/04/12	40	.01 to.06 .f1 to.f6
04	PT 21/22	48°12'52,349"	7°11'51,4365"	2013/04/13	37,5	.01 to.07 .f1 to.f7
05	R1	48°12'45,266"	7°11'48,1206"	2013/04/13	37,5	.01 to.06 .f1 to.f6
06	PH 15/16	48°12'42,2613"	7°11'58,604"	2013/04/14	37,5	.01 to.06 .f1 to.f6
07	Cut Plot	48°12'44,1525"	7°12'1,8074"	2013/04/14	40	.01 to.06 .f1 to.f6
08	R1/ Watchtower	48°12'46,1244"	7°11'53,1514"	2013/04/15	37,5	.01 to.06 .f1 to.f6
09	Humid Zone	48°12'44,2411"	7°12'11,5545"	2013/04/15	37,5	.01 to.06 .f1 to.f6
12	Springs 16/17	48°12'40,9749"	7°11'43,4266"	2013/04/17	37,5	.01 to.06 .f1 to.f6
13	Hirtzberg	48°12'32,0796"	7°11'34,9925"	2013/04/18	37,5	.01 to.06 .f1 to.f6
14	Spring Gneiss	48°12'55,2528"	7°11'48,6773"	2013/04/18	37,5	.01 to.06 .f1 to.f6
15	Above Springs	48°12'43,0026"	7°11'30,7657"	2013/04/19	37,5	.01 to.06 .f1 to.f6
16	North Ancient Snowfield	48°12'47,9833"	7°11'43,2572"	2013/05/20	37,5	.01 to.06 .f1 to.f6
19	Stream South Slope	48°12'41,0822"	7°11'52,0705"	2013/05/21	37,5	.01 to.06 and .020 .f1 to.f6 and .f13
22	Springs Collector	48°12'44,4081"	7°11'40,43"	2013/05/23	37,5	.01 to.06 .f1 to.f6
23	Pierre des 3 bans	48°12'35,5079"	7°11'24,8348"	2013/05/24	40	.01 to.06 .f1 to.f6

scale. The MRS measurements are collected at 16 stations in the Strengbach catchment (Fig. 1), which is the open-sky laboratory of the Observatoire Hydro-Géochimique de l'Environnement (OHGE, http://ohge.unistra.fr; CNRS/University of Strasbourg) [2]. MRS is a geophysical method directly sensitive to the water content of the subsurface. Details on the theory and the grounding fundaments of the method are available in [3]. The characteristics of each station of acquisition are summarized in Table 1. At each station, data are collected by setting an eight-shaped loop made by two squares on the ground surface (Fig. 1). The size and the location of the center of the loops for the different stations are listed in Table 1. The distances along the x (W-E direction) and y (N-S direction) directions of each corner of the eight-shaped loops to their center are reported in Table 2 for each station.

Table 2
Distance of the eight-shaped loops corners to the centre of each station. The lag-distances correspond to the location of the center minus the locations of the corners.

Station 1		Station 3		Station 4		Station 5	
Δx (m)	Δy (m)	Δx (m)	Δy (m)	Δx (m)	Δy (m)	Δx (m)	Δy (m)
-12.8	35.2	-6.9	39.4	-24.1	28.7	-9.7	36.2
22.4	48.1	-46.3	32.4	-52.8	4.6	26.5	45.9
35.2	12.8	-39.4	-6.9	-28.7	-24.1	36.2	9.7
-35.2	-12.8	39.4	6.9	28.7	24.1	-36.2	-9.7
-22.4	-48.1	46.3	-32.4	52.8	-4.6	-26.5	-45.9
12.8	-35.2	6.9	-39.4	24.1	-28.7	9.7	-36.2
Station 6		Station 7		Station 8		Station 9	
Δx (m)	Δy (m)	Δx (m)	Δy (m)	Δx (m)	Δy (m)	Δx (m)	Δy (m)
21.5	30.7	22.9	32.8	30.7	22.9	32.8	30.7
-9.2	52.2	-11.3	55.7	52.2	-11.3	55.7	52.2
-30.7	21.5	-32.8	22.9	21.5	-32.8	22.9	21.5
30.7	-21.5	32.8	-22.9	-21.5	32.8	-22.9	-21.5
9.2	-52.2	9.8	-55.7	-52.2	9.8	-55.7	-52.2
-21.5	-30.7	-22.9	-32.8	-30.7	-22.9	-32.8	-30.7
Station 12		Station 13		Station 14		Station 15	
Δx (m)	Δy (m)	Δx (m)	Δy (m)	Δx (m)	Δy (m)	Δx (m)	Δy (m)
12.8	35.2	12.8	35.2	-24.1	28.7	0	37.5
-22.4	48.1	-22.4	48.1	-52.8	4.6	37.5	37.5
-35.2	12.8	-35.2	12.8	-28.7	-24.1	37.5	0
35.2	-12.8	35.2	-12.8	28.7	24.1	-37.5	0
22.4	-48.1	22.4	-48.1	52.8	-4.6	-37.5	-37.5
-12.8	-35.2	-12.8	-35.2	24.1	-28.7	0	-37.5
Station 16		Station 19		Station 22		Station 23	
Δx (m)	Δy (m)	Δx (m)	Δy (m)	Δx (m)	Δy (m)	Δx (m)	Δy (m)
-12.8	35.2	9.7	36.2	-9.7	36.2	13.7	37.6
22.4	48.1	45.9	26.5	26.5	45.9	50.4	23.9
35.2	12.8	36.2	-9.7	36.2	9.7	37.6	-13.7
-35.2	-12.8	-36.2	9.7	-36.2	-9.7	-37.6	13.7
-22.4	-48.1	-45.9	-26.5	-26.5	-45.9	-51.3	-23.9
12.8	-35.2	-9.7	-36.2	9.7	-36.2	-13.7	-37.6

For each station, the data files are gathered in a .zip file that contains a data and a figure folder. A .pdf metadata file gathers all the information about each station. In the data folder, a .inp file summarizes the parameters of each acquisition corresponding to the raw data files (.0#) that are provided together with the filtered data files (.f#), with # the file number. The files follow the SAMOVAR 11.62 format. For an easier use of the data, a .mrm file is also provided which contains information on the kernel matrix of the MRS sounding. Different .mrm files are provided, depending on the size of the loop.

As the SAMOVAR software is not freely distributed, the MRS toolbox described in [4] can also be used; it allows to open and process the raw data, compute a 1D kernel, and perform inversion.

Here is a brief description of the files formats:

Each line of the .inp file corresponds to one of the filtered files, then the number of pulse injected is provided, followed by the pulse frequency (Hz), and finally the moment pulse sequence setup (injected current intensity multiplied by duration, A.ms).

In the field, the acquisition can be divided in six steps:

1. Noise recording.
2. Pulse 1 injection.
3. Signal 1 recording.
4. Pulse 2 injection.
5. Signal 2 recording.
6. Signal 3 recording.

Between each step, the system needs for a downtime to let the electronics of the instrument to switch from the acquisition to the injection mode and vice-versa. Each .0# file supplies the results of the stacked data and corresponds to one of the injected pulses of various moments. The first line of the file provides a series of numbers corresponding to:

1. The clock frequency f (Hz).
2. The phase shift of the generator (degree).
3. The phase shift of the amplifier (degree).
4. The antenna type: 1: circular loop, 2: square loop, 3: eight shape circular loop, 4: eight shape square loop.
5. The average noise evaluation (nV).
6. The Udc/dc (V).
7. The coefficient of amplification.
8. The antenna impedance for the generation of the pulse (ohm).
9. The number of lines in the data file.

The second line contains a second series of numbers corresponding to:

1. The number of readings of the noise.
2. The pause length T_{pause1} between the noise recording and the first pulse; the pause duration is $T_{pause1}.(0.25/f)$ ms.
3. The duration of the first injected pulse $T_{injection1}$; the pulse duration is $T_{injection1}.(0.4/f)$ ms.
4. The pause length T_{pause2} between the first pulse and the first signal recording; the pause duration is $T_{pause2}.(0.25/f)$ ms
5. The number N_1 of readings of the signal 1; the recording time is $N_1.(4/f)$ ms.
6. The pause length T_{pause3}; the pause duration is $T_{pause3}.(0.25/f)$ ms.
7. The duration of the second pulse $T_{injection2}$; the pulse duration is $T_{injection2}.(4/f)$ ms.
8. The pause length T_{pause4}; the pause duration is $T_{pause4}.(0.25/f)$ ms.
9. The number N_2 of readings of the signal 2;the recording time is $N_2.(4/f)$ ms.
10. The pause length T_{pause5}; the pause duration is $T_{pause5}.(0.25/f)$ ms.
11. The number N_3 of readings of signal 3; the recording time is $N_3.(4/f)$ ms.

Then, 13 columns provide the readings of the noise, the injected pulses, and the signals:

1. Recording time (ms).
2. Noise of the in-phase component X (nV).
3. Noise of the out-of-phase component Y (nV).
4. Pulse 1 X current (A).
5. Pulse 1 Y current (A).
6. Signal 1 X (nV).
7. Signal 1 Y (nV).
8. Pulse 2 X current (A).
9. Pulse 2 Y current (A).
10. Signal 2 X (nV).
11. Signal 2 Y (nV).
12. Signal 3, also called spin echo (SE), X (nV).
13. Signal 3, also called spin echo (SE) Y (nV).

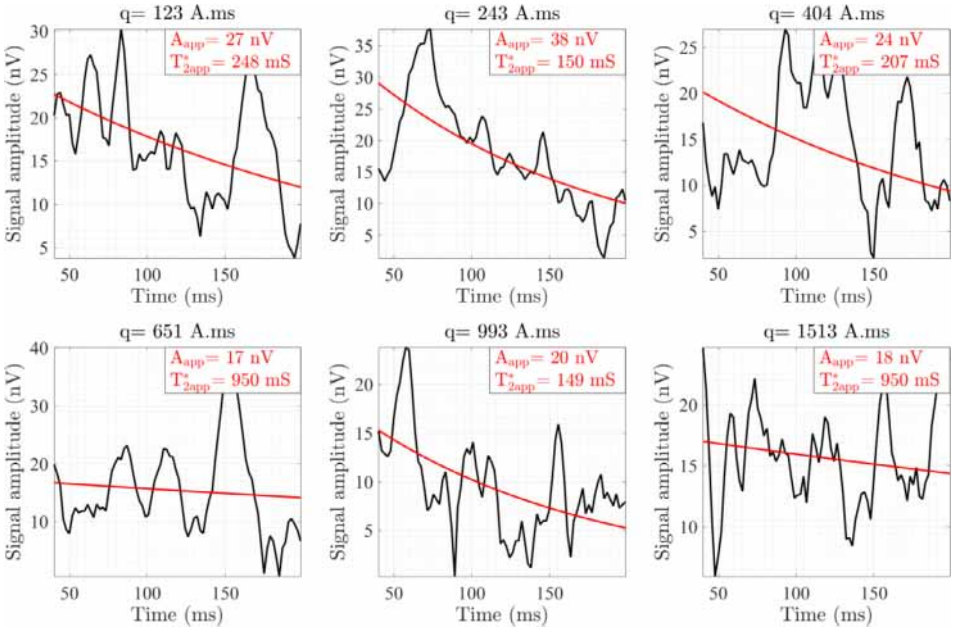

Fig. 2. Recorded signal envelope at station 1 (black curve) and decaying exponential model of the signal envelope with amplitude A_{app} and a characteristic time T^*_{2app} (red curve).

The raw data are filtered and the filtered signals are recorded in the .f# files. The first line provides the number of lines in the file, then the signals are presented in 11 columns:

1. Acquisition time (ms).
2. Free induction decay (FID)1 in-phase component X of the signal (nV).
3. FID1 out-of-phase component Y of the signal (nV)
4. Filtered noise recorded in X (nV).
5. Filtered noise recorded in Y (nV).
6. FID1 X filtered signal (nV).
7. FID1 Y filtered signal (nV).
8. FID2 X filtered signal (nV).
9. FID2 Y filtered signal (nV).
10. SE X filtered signal (nV).
11. SE Y filtered signal (nV).

In the paper [1], the signals recorded were selected so they correspond to the weaker injected pulses that are the data the most sensitive to the shallow properties of the subsurface. The files selected in [1] are listed in Table 1 and their corresponding signals are presented in Figs. 2–17. From these signals, an apparent relaxation time T^*_{2app} is deduced as detailed in the following to estimate the median relaxation time at each station that are presented in Table 3. Details on the significance and the computation of T^*_{2NIHM} and T^*_{2Deep} values are given in [1]. The dataset is hosted in the H+ data base (http://hplus.ore.fr/en/) with a direct access (http://hplus.ore.fr/en/lesparre-et-al-2020-joh-data)

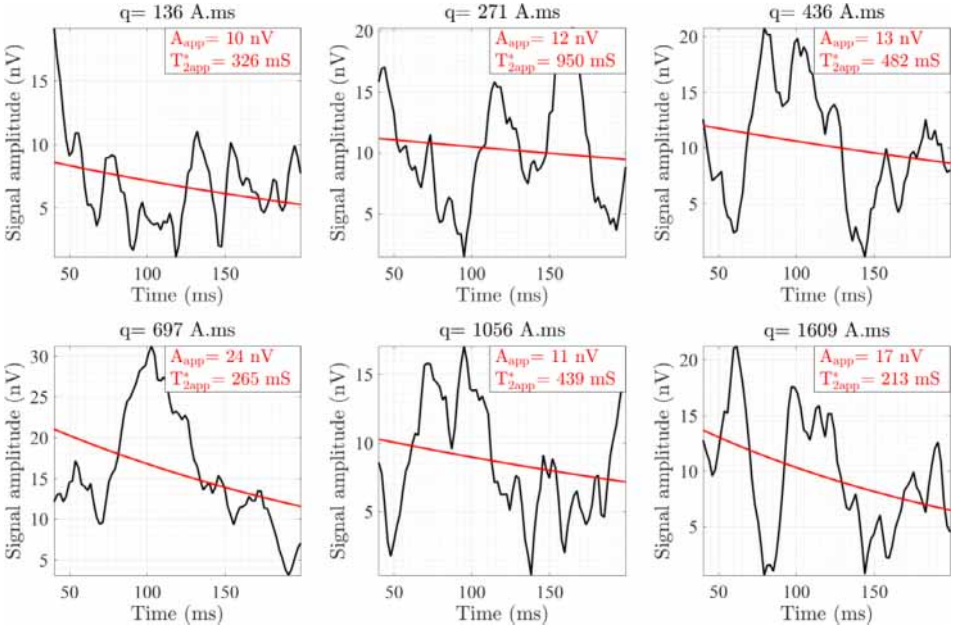

Fig. 3. Recorded signal at station 3.

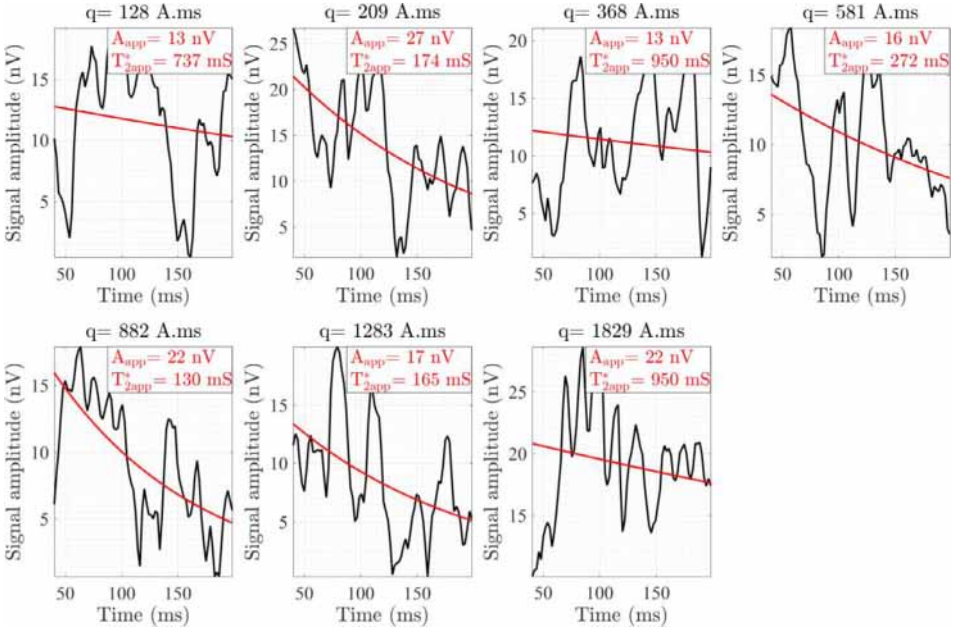

Fig. 4. Recorded signal at station 4.

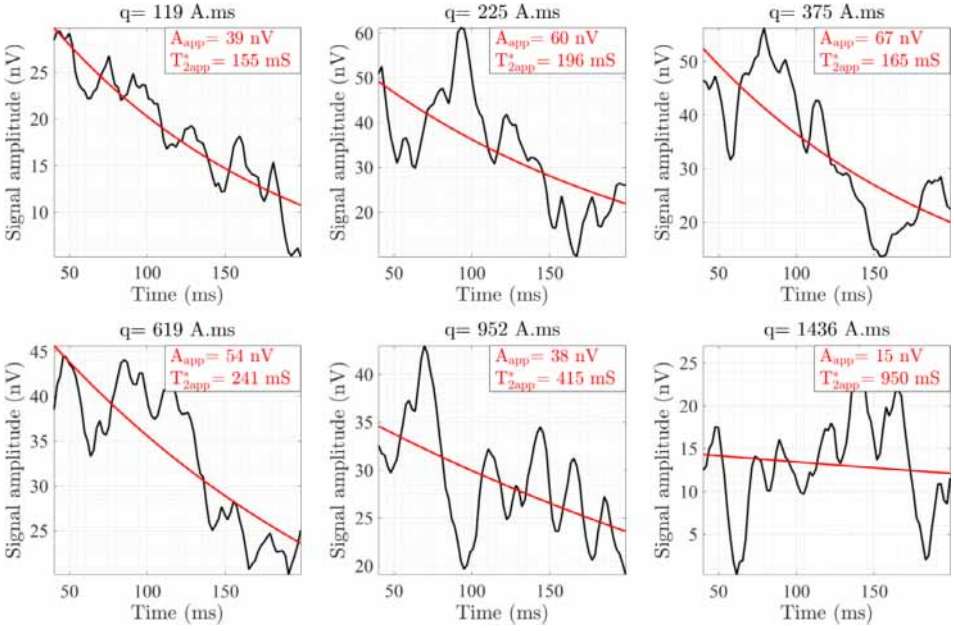

Fig. 5. Recorded signal at station 5.

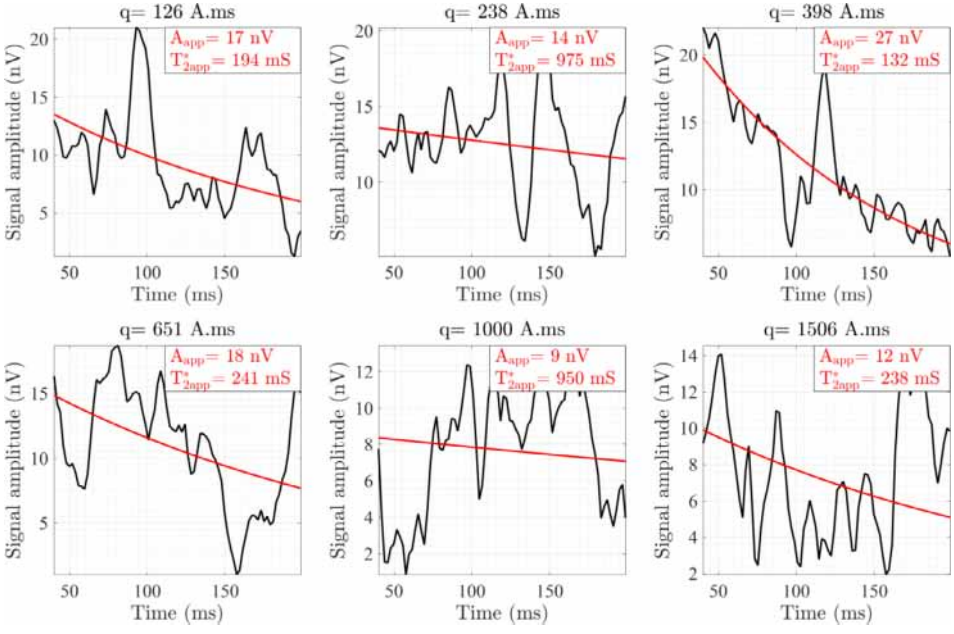

Fig. 6. Recorded signal at station 6.

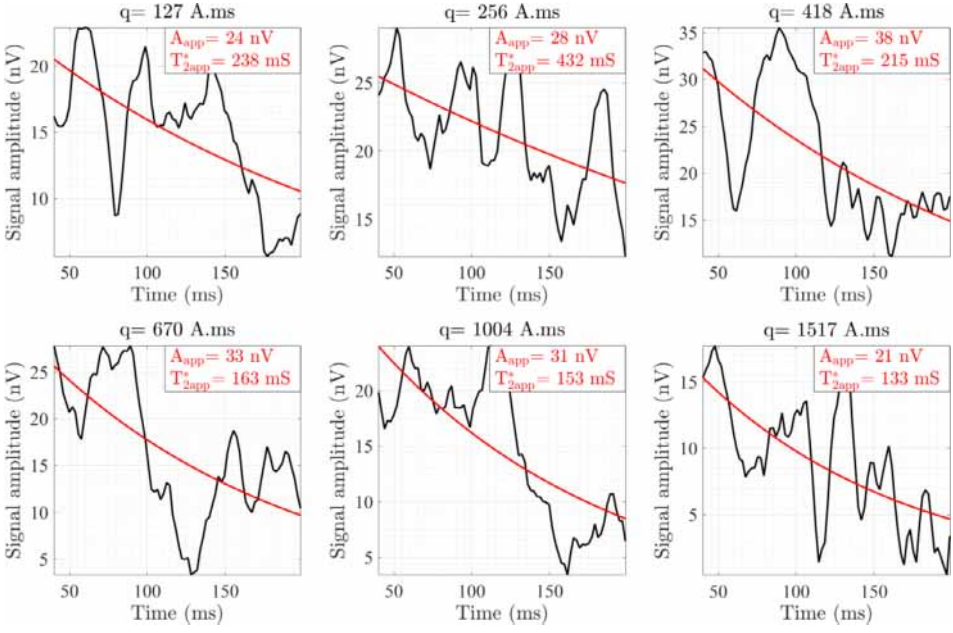

Fig. 7. Recorded signal at station 7.

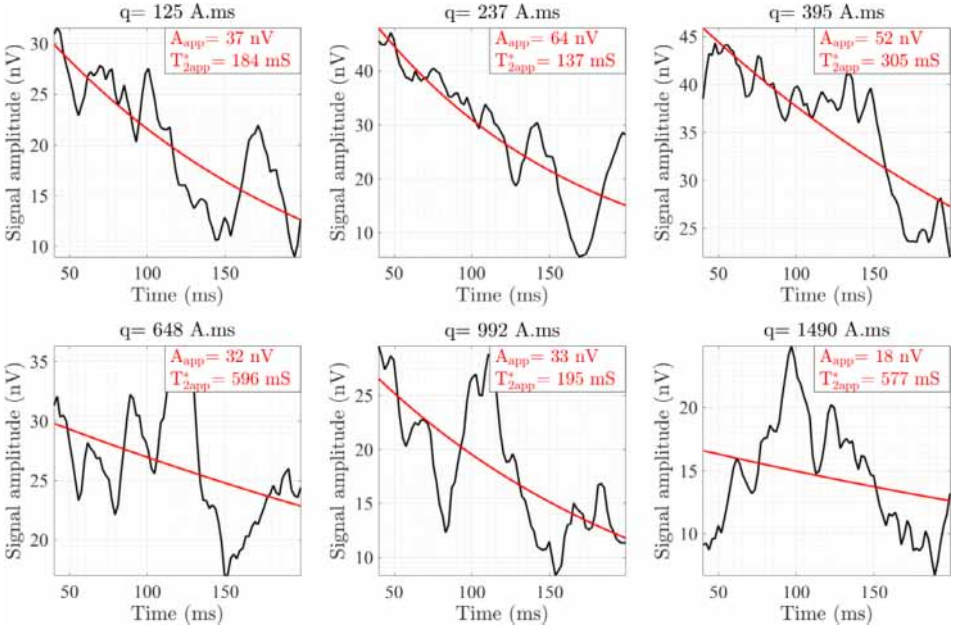

Fig. 8. Recorded signal at station 8.

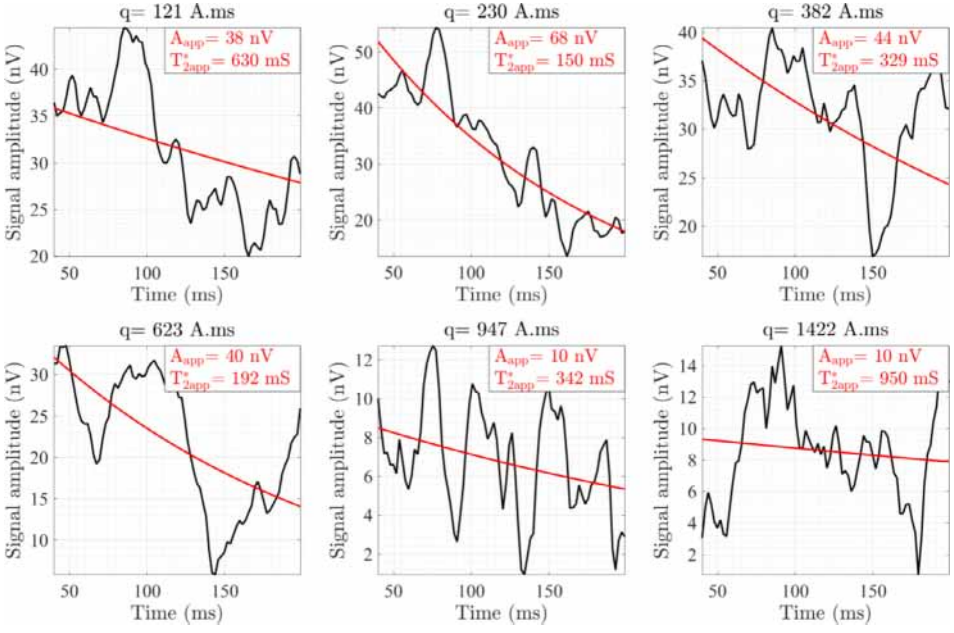

Fig. 9. Recorded signal at station 9.

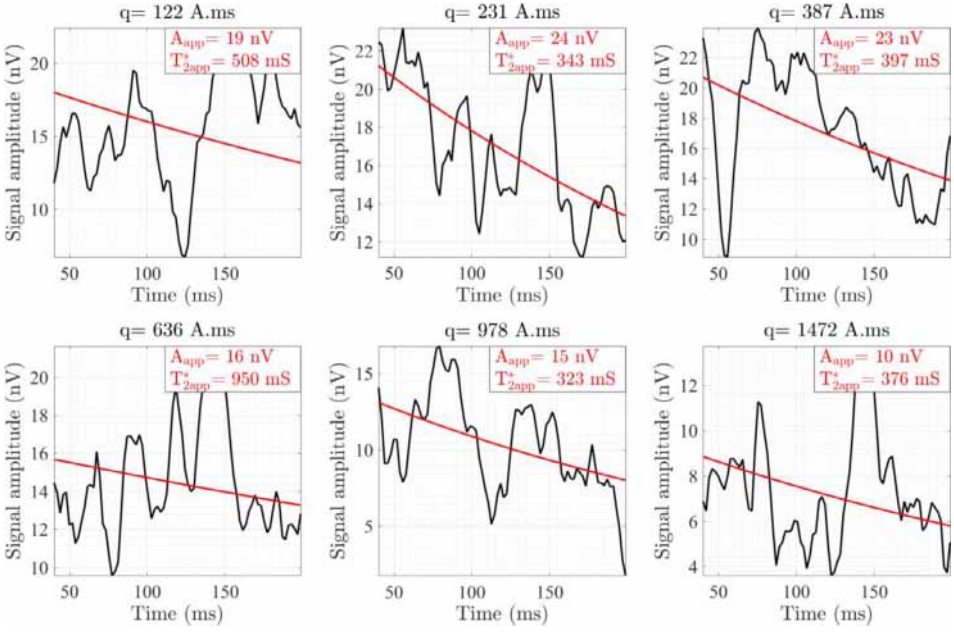

Fig. 10. Recorded signal at station 12.

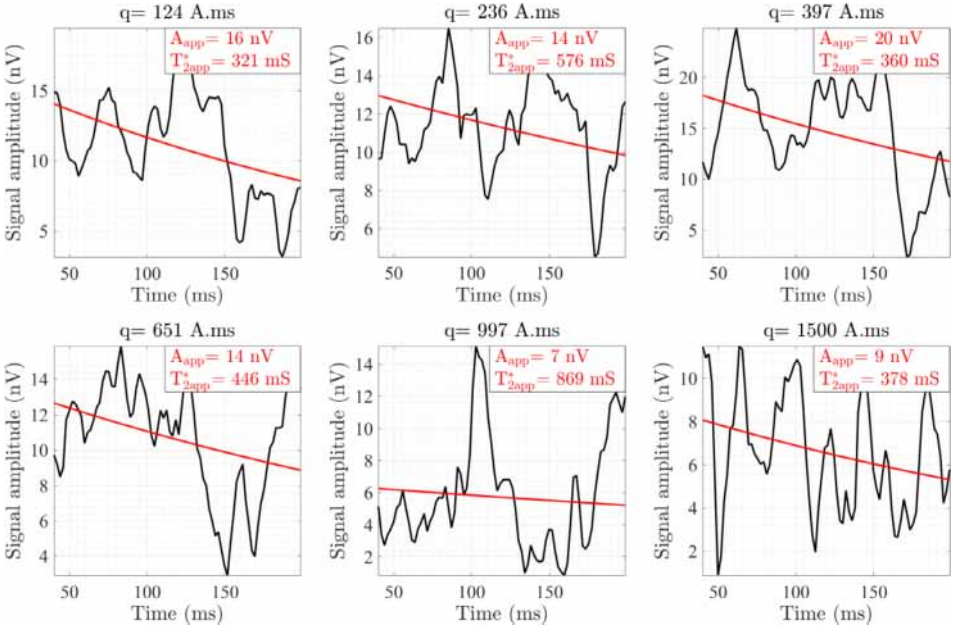

Fig. 11. Recorded signal at station 13.

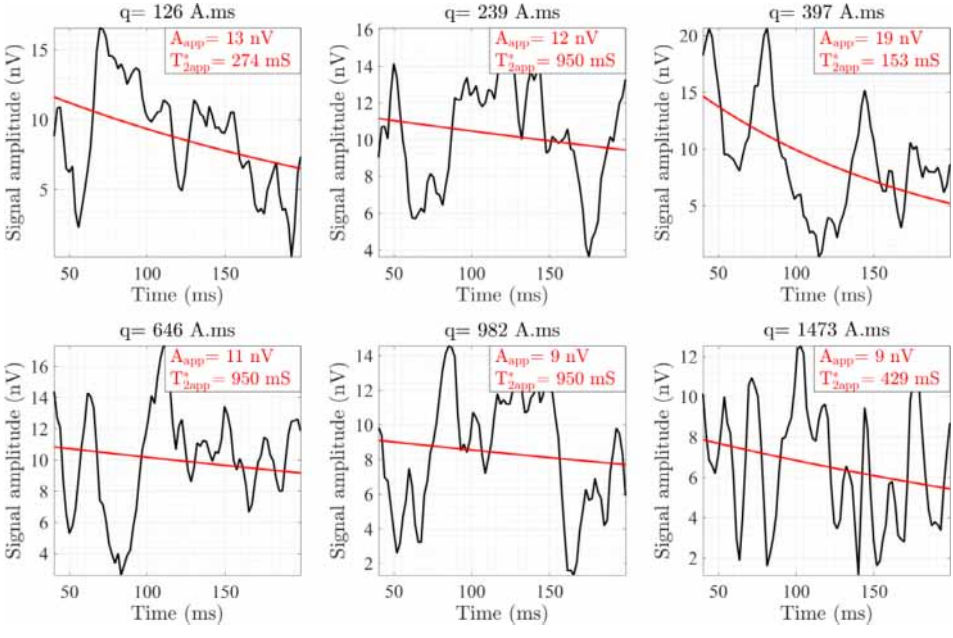

Fig. 12. Recorded signal at station 14.

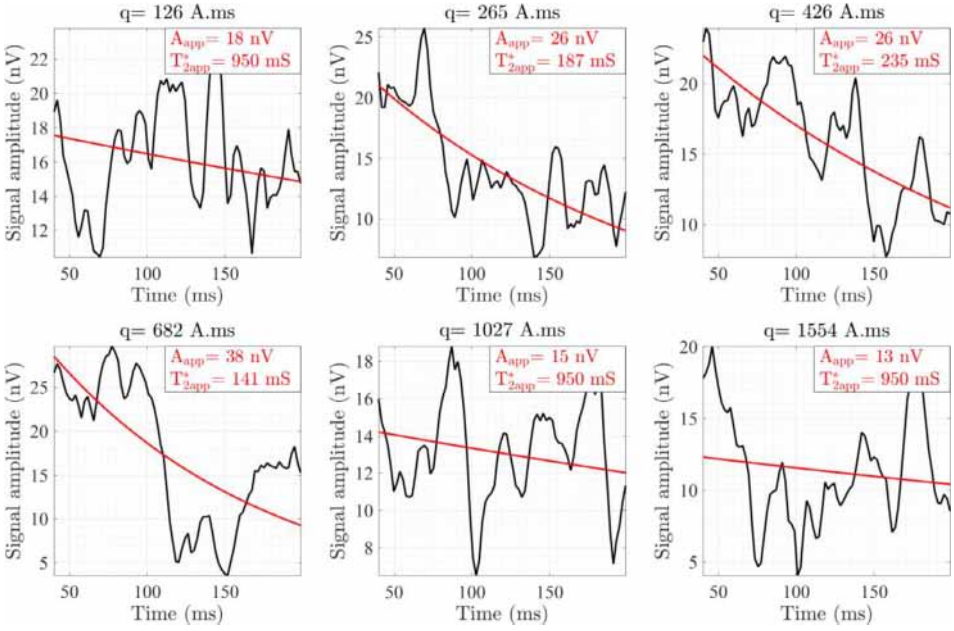

Fig. 13. Recorded signal at station 15.

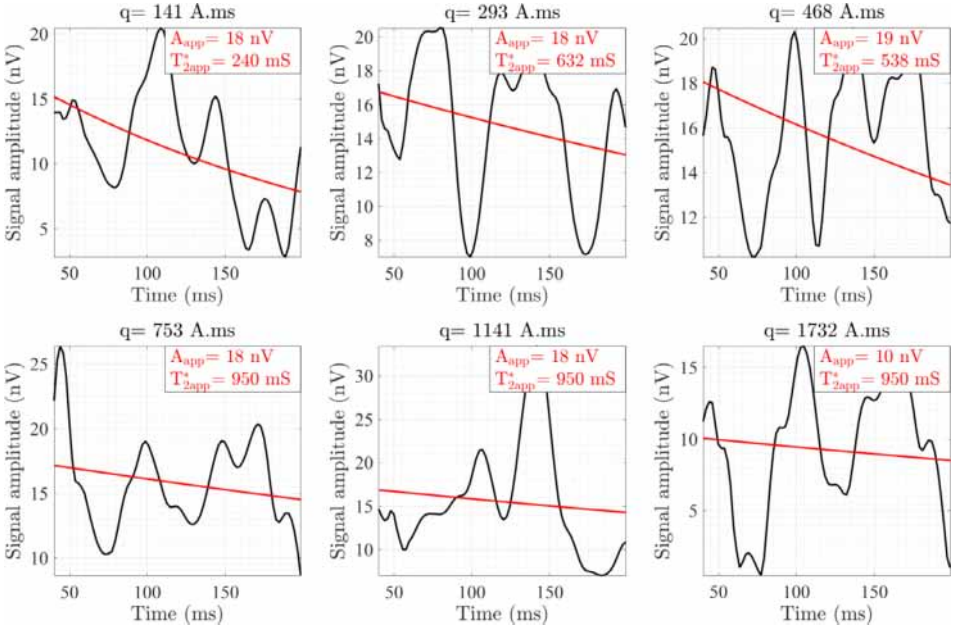

Fig. 14. Recorded signal at station 16.

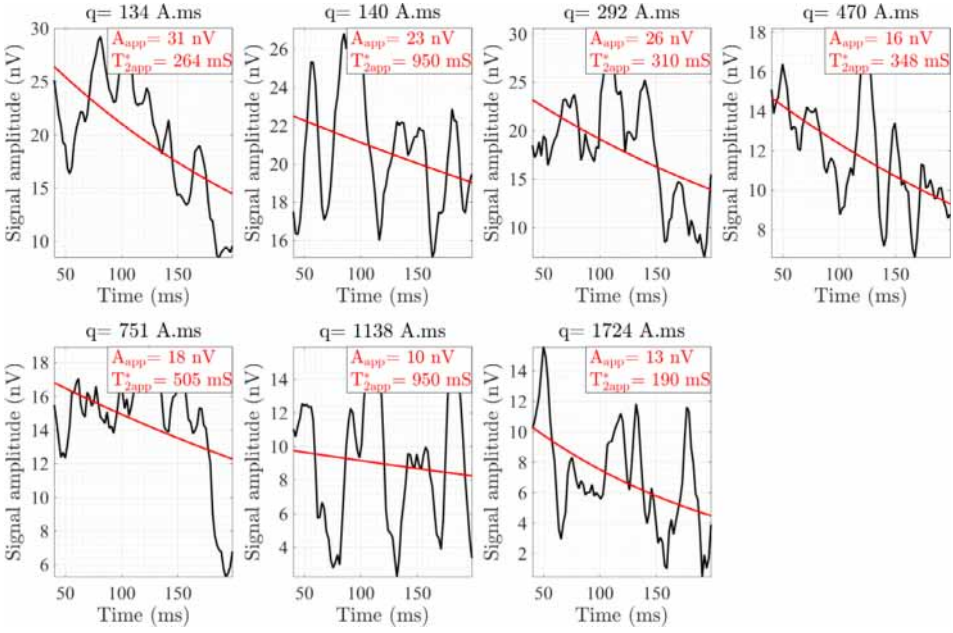

Fig. 15. Recorded signal at station 19.

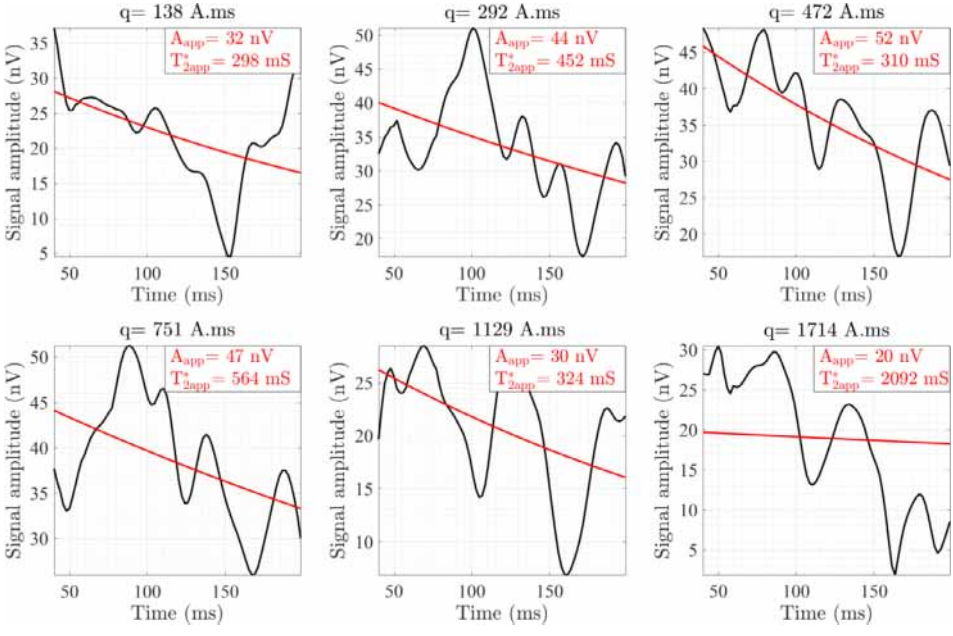

Fig. 16. Recorded signal at station 22.

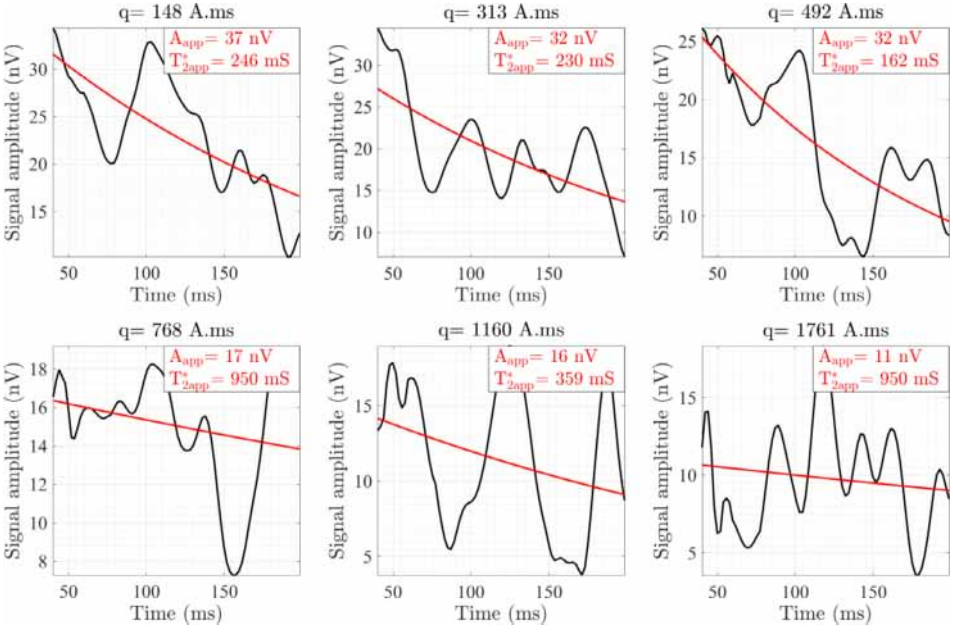

Fig. 17. Recorded signal at station 23.

Table 3
Values of the T_2^* characteristic times in the exponential decays of the MRS signals T^*_{2Med} corresponds to the median of the $T^*_{2app}(q)$ values estimated from the fit of Eq. 1 on the observed temporal signal T^*_{2NIHM} is the value estimated in the two layers of the shallow aquifer T^*_{2Deep} is the value estimated in the weathered bedrock compartment beneath the aquifer (see Fig. 5 in [1]

Station	T^*_{2Med} (ms)	T^*_{2NIHM} (ms)	T^*_{2Deep} (ms)
1	227	305	1137
3	383	77	1914
4	272	241	1211
5	218	249	1091
6	240	119	1199
7	189	326	189
8	250	133	1251
9	336	325	1109
12	386	527	1476
13	412	1752	1325
14	689	138	690
15	592	248	2962
16	791	253	3956
19	348	1304	225
22	388	645	188
23	303	287	406

2. Experimental Design, Materials, and Methods

Acquisition protocols follow the free induction decay (FID) scheme described in [3]. Here, only one pulse is injected after the noise measurement, then the signal is recorded. Each pulse is stacked 200 to 300 times. After a time out of 40 ms, the signals are recorded with a sampling rate of 2 ms and over a duration between 205 and 466 ms. However, for the analysis performed

in [1], only the first 162 ms (after the time out) of the recording were kept because the long-time measurements are much more sensitive to the ambient noises.

Data are analyzed and filtered using the SAMOVAR-11.62 software package developed at the Institut de Recherche pour le Développement (IRD, France). First a band-pass filter is applied around the Larmor frequency, and then a filter removing the 50 Hz noise is applied, except if the Larmor frequency is close to a 50 Hz harmonic.

The filtered MRS measurements are then post-processed by seeking, for each pulse q, the best model $W(q,t)$ for the envelope of the signal measured over time as:

$$W(q,t) = A_{app}(q)\exp\left(-t/T^*_{2app}\right) \quad (1)$$

where A_{app} and T^*_{2app} are the sought parameters. For each pulse of each station, the computed $W(q,t)$ are represented in red Figs. 2–17. From this analysis, the median of T^*_{2app} is determined at each station, as reported in in Table 3.

The kernel matrices provided in the .mrm files are computed with a Larmor frequency of 2040 Hz, an inclination of the geomagnetic field of 65°, and a resistivity of the subsurface of 1000 ohm.m. These files can be used directly when analyzing the data with SAMOVAR-11.62 or the MRS toolbox described in [4].

The location of the loops is determined with a handheld GPS, the precision of stations location being of ±5 m. The distances between the loop corners and their center are determined in view of the size and the orientation of the squares composing the eight-shaped loops.

Acknowledgments

The MRS acquisition campaign was funded by CRITEX, INSU, and REALISE projects. The authors acknowledge Daniel Sultana (LTHE), Troels Thomsen (LTHE), Sylvain Benarioumlil (OHGE), and Valentin Gondy (OHGE) for their help in the fieldworks. OHGE is part of the OZCAR research infrastructure (http://www.ozcar-ri.org). The authors would also like to thank the OZCAR network for the scientific animation that stimulated this work and the ANR HYDROCRIZSTO-15-CE01-0010-02 project.

Conflict of interest

The authors declare that they have no known competing financial interests or personal relationships which have, or could be perceived to have, influenced the work reported in this article.

Supplementary materials

Supplementary material associated with this article can be found, in the online version, at doi:10.1016/j.dib.2020.105708.

References

[1] N. Lesparre, J.-F. Girard, B. Jeannot, S. Weill, M. Dumont, M. Boucher, D. Viville, M.-C. Pierret, A. Legchenko, F. Delay, Magnetic resonance sounding measurements as posterior information to condition hydrological model parameters: Application to a hard-rock headwater catchment, J, Hydrol 587 (2020) 124941 https://doi.org/10.1016/j.jhydrol.2020.124941.

[2] M.C. Pierret, S. Cotel, P. Ackerer, E. Beaulieu, S. Benarioumlil, M. Boucher, R. Boutin, F. Chabaux, F. Delay, C. Fourtet, P. Friedmann, B. Fritz, S. Gangloff, J.-F. Girard, A. Legtchenko, D. Viville, S. Weill, A. Probst, The Strengbach catchment: A multidisciplinary environmental sentry for 30 years, Vadose Zone J 17 (2018) 1 https://doi.org/10.2136/vzj2018.04.0090.

[3] A. Legchenko, P. Valla, A review of the basic principles for proton magnetic resonance sounding measurements, J. Appl. Geophys. 50 (2002) 3–19 https://doi.org/10.1016/S0926-9851(02)00127-1.
[4] M. Müller-Petke, M. Braun, M. Hertrich, S. Costabel, J. Walbrecker, MRSmatlab—A software tool for processing, modeling, and inversion of magnetic resonance sounding dataMRSmatlab, Geophysics 81 (2016) WB9–WB21 https://doi.org/10.1190/geo2015-0461.1.